Head, J. F., & Perry, S. V. (1974) *Biochem. J. 137*, 145-154.
Head, J. F., Masure, H. R., & Kaminer, B. (1982) *FEBS Lett. 137*, 71-74.
Johnson, J. D., & Wittenauer, L. A. (1983) *Biochem. J. 211*, 473-479.
Katzenellenbogen, J. A., Johnson, H. J., Carlson, K. E., & Myers, H. N. (1974) *Biochemistry 13*, 2986-2994.
Klee, C. B., & Vanaman, T. C. (1982) *Adv. Protein Chem. 35*, 213-321.
Klevit, R. E., Levine, B. A., & Williams, R. J. P. (1981) *FEBS Lett. 123*, 25-29.
Krebs, J. (1981) *Cell Calcium 2*, 295-311.
Krebs, J., & Carafoli, E. (1982) *Eur. J. Biochem. 124*, 619-627.
Kretsinger, R. H. (1975) in *Calcium Transport in Contraction and Secretions* (Carafoli, E., Clementi, F., Drabikowski, W., & Margreth, A., Eds.) pp 469-478, Elsevier/North-Holland, Amsterdam.
Laemmli, U. K. (1970) *Nature (London) 227*, 680-685.
La Porte, D. C., Wierman, B. M., & Storm, D. R. (1980) *Biochemistry 19*, 3814-3819.
Levin, R. M., & Weiss, B. (1977) *Mol. Pharmacol. 13*, 690-697.
Lowry, O. H., Rosebrough, N. J., Farr, A. L., & Randall, R. J. (1951) *J. Biol. Chem. 193*, 265-275.
Newton, D. L., Oldenwurtel, M. D., Krinks, M. H., Shiloach, J., & Klee, C. B. (1983) *J. Biol. Chem.* (in press).
Norman, J. A., Drummond, A. H., & Moser, P. (1979) *Mol. Pharmacol. 16*, 1089-1094.
Seamon, K. B., & Kretsinger, R. H. (1983) in *Metal Ions in Biology* (Spiro, T. G., Ed.) Vol. VI, Wiley, New York (in press).
Szebenyi, D. M. E., Obendorf, S. K., & Moffat, K. (1981) *Nature (London) 294*, 327-332.
Tanaka, T., & Hidaka, H. (1980) *J. Biol. Chem. 255*, 11078-11080.
Teo, T. S., & Wang, J. H. (1973) *J. Biol. Chem. 248*, 5950-5955.
Thulin, E., Andersson, A., Drakenberg, T., Forsén, S., & Vogel, H. J. (1983) *Biochemistry* (in press).
Vogel, H. J., Lindahl, L., & Thulin, E. (1983) *FEBS Lett. 157*, 241-246.
Walsh, M., Stevens, F. C., Kuznicki, J., & Drabikowski, W. (1977) *J. Biol. Chem. 252*, 7440-7443.
Watterson, D. M., Sharief, F., & Vanaman, T. C. (1980) *J. Biol. Chem. 255*, 962-975.

Aqueous Solution Structure of an Intercalated Actinomycin D-dATGCAT Complex by Two-Dimensional and One-Dimensional Proton NMR†

Stephen C. Brown, Kary Mullis, Corey Levenson, and Richard H. Shafer*

ABSTRACT: Two-dimensional NOESY and COSY ^{1}H NMR techniques have been employed to determine the conformation of the complex formed by actinomycin D and the hexanucleoside pentaphosphate dATGCAT. One-dimensional NOE experiments in H_2O confirmed the intact nature of the oligonucleotide double helix within the complex. The drug chromophore was intercalated between the GC base pairs, with the pentapeptide lactones nestled in the minor groove. No significant conformational change of the pentapeptide lactones between bound and free drug was observed.

The actinomycins (Mauger, 1980) are a class of antitumor antibiotics that inhibit DNA-directed RNA synthesis in both eucaryotic and procaryotic cells by binding to the DNA template. Actinomycin D (Figure 1) was shown to be one of the most effective of the natural analogues, which share the same chromophore structure but differ only by amino acid substitutions in the pentapeptide lactone moieties. The inhibition of RNA synthesis was shown to correlate less directly with binding constants than with rates of association and dissociation from DNA (Muller & Crothers, 1968), which are quite slow ($\sim 10^{-3}$ s^{-1}) compared to other typical DNA binding drugs such as ethidium bromide and daunomycin (10^1-10^3 s^{-1}). The relatively slow rates have been attributed to conformational changes in the pentapeptide lactones (Muller & Crothers, 1968; Shafer et al., 1980; Brown et al., 1982; Mirau & Shafer, 1982) or in the nucleic acid (Sobell, 1974).

A crystal structure of actinomycin D (ACTD)[1] complexed with deoxyguanosine has been published (Jain & Sobell, 1972), from which a model of ACTD bound to the hexanucleoside pentaphosphate duplex dATGCAT was proposed (Sobell & Jain, 1972). NMR data obtained from binding ACTD to various dinucleotides (e.g., dCpG, dGpC, etc.), mononucleotides (Reinhardt & Krugh, 1977; Krugh & Chen, 1975; Patel, 1974a), and oligomers (Patel, 1974b; Patel et al., 1981; Reid et al., 1983) have been interpreted to be consistent with the proposed model. However, the mono- and dinucleotide systems investigated showed fast kinetics (Davanloo & Crothers, 1976) and may not be truly representative of the slowly associating/dissociating binding mode directly correlated to RNA synthesis inhibition. These previous NMR

† From the Department of Pharmaceutical Chemistry, School of Pharmacy, University of California, San Francisco, California 94143 (S.C.B. and R.H.S.), and the Cetus Corporation, Emeryville, California 94608 (K.M. and C.L.). *Received October 20, 1983.* This research was supported by U.S. Public Health Service Grant CA 27343 awarded by the National Institutes of Health, the Cetus Corp., and the University of California Intercampus Activity Fund.

[1] Abbreviations: ACTD, actinomycin D; COSY, ^{1}H two-dimensional *J*-correlation NMR; NOESY, ^{1}H two-dimensional NOE correlation NMR in the pure absorption mode; TSP, sodium 3-(trimethylsilyl)-tetradeuteriopropionate; EGTA, ethylene glycol bis(β-aminoethyl ether)-*N,N,N',N'*-tetraacetic acid; FID, free induction decay; NMR, nuclear magnetic resonance; TLC, thin-layer chromatography; Nmv, L-*N*-methylvaline; Thr, L-threonine; Dva, D-valine; Pro, L-proline; Sar, sarcosine; TOE, truncated driven nuclear Overhauser effect; HPLC, high-pressure liquid chromatography; DP, data point.

0006-2960/84/0423-0403$01.50/0

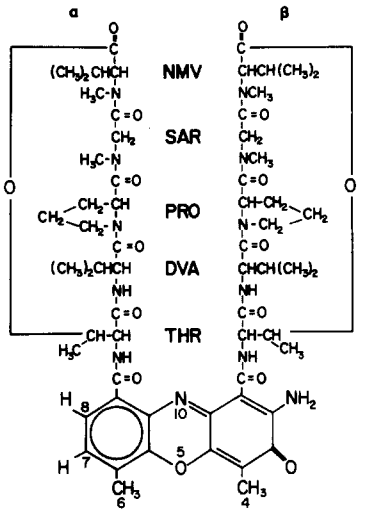

FIGURE 1: Actinomycin D structure. The benzenoid (b) and quinoid (q) parts of the phenoxazone chromophore are on the left and right side, respectively. In the crystal structure there is a pseudo-C^2 axis through atoms N10 and O5 of the chromophore (Jain & Sobell, 1972).

studies have generally been limited to observations of several resonances in the nucleotide or drug and have not addressed the issue of what structural changes may be responsible for the slow kinetics. Recently, a ^1H NMR investigation of the complex ACTD–dAGCT (1:2) demonstrated by NOE effects that the ACTD chromophore was intercalated, but it provided little information concerning the conformation of the ACTD pentapeptides or the nucleic acid residues apart from the intercalation site (Reid et al., 1983). A recent crystal structure of an ACTD–dGpC (1:2) complex revealed an unusual pseudointercalated geometry (Takusagawa et al., 1982) that may exist in solution.

The development of two-dimensional NMR techniques has expanded the possibilities of resolving, assigning, and measuring NOE's in crowded spectra (Wüthrich et al., 1982). Several solution structures of relatively large molecules have been elucidated with these techniques [e.g., Braun et al. (1981)]. This paper has extended these techniques to the determination of structural features in a noncovalently bound complex of ACTD and the hexanucleoside pentaphosphate dATGCAT. In addition, one-dimensional NOE measurements in H_2O have revealed that the oligonucleotide duplex remains essentially intact, a result incompatible with a pseudointercalated structure where the central GC base pairs have "swung out" of the helix. The oligonucleotide dATGCAT was selected for study for several reasons: (1) it contains only one unique strong binding site for ACTD, (2) it is long enough to interact with the pentapeptide lactones of ACTD, and (3) the kinetics of ACTD–dATGCAT association are slow and mimic the kinetics of ACTD–DNA association (unpublished results).

Materials and Methods

ACTD was a generous gift from Merck Sharpe & Dohme, and its purity was checked by TLC and NMR. Buffer reagents were obtained from Sigma. TSP and D_2O were obtained from Wilmad. dATGCAT was synthesized by standard triester techniques (Narang et al., 1980), and its purity was checked by ^1H NMR, ^{31}P NMR, HPLC, and base composition analysis. Solutions for NMR experiments were made up in a phosphate buffer (100 mM phosphate, 180 mM NaCl, 0.2 mM EGTA, pH 7.0). ACTD was dissolved to a concentration of 4.0 mM; the solution was lyophilized twice and taken up in an equal volume of D_2O. The complex was formed by the addition of integral stoichiometric ratios of solid dATGCAT (Na^+ salt). Individual samples contained (1) ACTD alone, (2) ACTD–dATGCAT (1:1), (3) ACTD–dATGCAT (1:2), and (4) ACTD–dATGCAT (1:4). These were lyophilized in the NMR tube and taken up again into an equal volume of D_2O to which solid TSP was added for an internal chemical shift standard.

NMR Experimental Parameters. All experiments, unless otherwise indicated, were done on a 500-MHz Nicolet 1280 instrument at the University of California, Davis, CA. The 90° pulse time was 11 μs. Sample T_1 values ranged from 0.5 to 2.3 s, so the delay between acquisitions was set to 5 s, unless stated otherwise. The carrier was set to the frequency of the residual solvent peak, which was suppressed by using a phase-cycled soft pulse (t_π = 120 ms) during the acquisition delay.

(A) Saturation-transfer experiments were done on the 240-MHz home-built wide-bore NMR at the University of California, San Francisco, equipped with Nicolet 1180 software and a 293B pulse programmer. The decoupler was used at the minimum power necessary to ensure selectivity. Resonances of both the complex and the previously assigned resonances of the duplex dATGCAT (unpublished data) were irradiated with the ACTD–dATGCAT (1:4) sample. The temperature was controlled at 45 °C, where peaks were observed to be at slow exchange, but saturation transferred with a 0.5-s preirradiation. Spectra were acquired by using the interleave mode with appropriate off-resonance controls and the FID's subtracted to obtain difference spectra.

(B) One-dimensional NOE observations of the dATGCAT imino proton resonances were done in the identical buffer with 90% H_2O/10% D_2O. The temperature was controlled at 0 °C to minimize exchange with solvent and maximize NOE effects. A jump and return (Plateau & Gueron, 1982) sequence was used to suppress the H_2O signal, with a decoupler preirradiation of 0.5–1.0 s. The decoupler power was set lower than that required for complete saturation of resonances, in order to minimize dispersion.

(C) Two-dimensional COSY spectra (Bax et al., 1981) were acquired by using 4K data points in the t_2 dimension and 200 acquisitions in the t_1 dimension. FID's were apodized in the t_2 dimension by a double exponential and in the t_1 dimension by a sine bell, yielding after transformation a 2K × 512 matrix of real points with a resolution of 4 Hz/DP (ω_2) and 16 Hz/DP (ω_1). The sample temperature was regulated at 15 °C.

(D) Two-dimensional NOESY spectra were acquired in the pure absorption mode (States et al., 1982) with 4K data points in the t_2 dimension (64 acquisitions each), stored in alternate blocks, and 200 FID's collected in the t_1 dimension. A mixing time (τ_m) of 200 ms was found to yield optimum signal to noise ratios. No effects due to spin diffusion were evident at observation times less than ~0.5 s by TOE experiments (Wagner & Wüthrich, 1979). FID's were apodized in the t_2 dimension by Gaussian multiplication and in the t_1 dimension by double exponential multiplication to enhance resolution, yielding after transformation a 1K × 1K matrix of real points with digital resolution of 5.8 Hz/DP. The sample temperature was regulated at 15 °C.

Results and Discussion

Proton NMR spectra of ACTD, dATGCAT, and their complex ACTD–dATGCAT (1:2) are shown in Figure 2. Resonances have been assigned by use of various techniques. Previous work (Angerman et al., 1972) had established many proton assignments for ACTD in aqueous solution by binary solvent titrations from deuteriobenzene through deuterio-

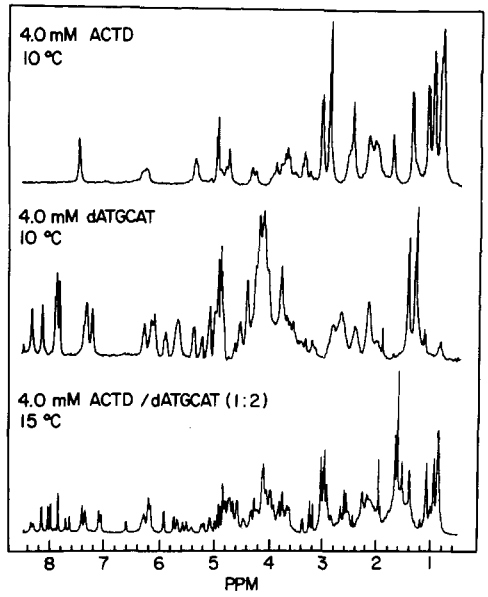

FIGURE 2: 500-MHz ^{1}H NMR spectra of actinomycin D, dATGCAT, and their complex ACTD–dATGCAT (1:2) in phosphate buffer/D_2O, 64 transients each, with the residual HDO peak suppressed by irradiation during acquisition delay.

methanol to D_2O. These assignments were confirmed and extended by COSY and NOESY spectra. Amino acid residues on the pentapeptide lactones were identified by their characteristic spin systems (sarcosine, AX; threonine, A_3MX; proline, AA'MM'NN'X; valine, A_3B_3MX) appearing in the COSY spectrum of ACTD. Assignments for the chromophoric methyl groups and protons H7 and H8 were confirmed by transient NOE measurements (TOE) (Wagner & Wüthrich, 1979).

Assignment of the two valine spin systems proceeded as follows by measurement of NOE buildup rates. The large doublet (δ = 3.09, 3.06 ppm) and the singlet (δ = 2.94 ppm) have been previously assigned to *N*-methylvaline (N-CH_3) and sarcosine (N-CH_3) protons, respectively (Angerman et al., 1972). An NOE was observed to one of the valine H_α protons upon irradiation of the downfield doublet. Irradiation of the upfield singlet produced NOE's to the sarcosine H_α protons. Irradiation of the sarcosine H_α protons produced NOE's to both the doublet and the singlet. This pattern of NOE's confirmed the assignment of the N-CH_3 groups and established the identities of the two valine spin systems. The assignments of Angerman et al. (1972) were confirmed except for the following: Nmv H_α (3.35 ppm), Dva H_α (3.60), Sar $H_{\alpha 2}$ (4.23, 4.31), Sar $H_{\alpha 1}$ (4.8, 4.9), Thr H_α (4.7, 5.0), Thr H_β (5.35), Pro $H_{\beta 2}$ (2.62), Pro $H_{\beta 1,\gamma}$ (~2.05), and Pro H_δ (3.8, 3.9).

The Thr $H_{\alpha 2}$ resonance was difficult to observe in the presence of trace amounts of H_2O, but cross peaks could be seen in the COSY and NOESY spectra when the sample was rigorously exchanged with "100%" D_2O. (Assignment of resonances to the α or β pentapeptide could not be done due to their superposition from the semi-C_2 symmetry of the molecule.) The structure of ACTD in solution appears similar to that observed in the crystal structure (Jain & Sobell, 1972) when relative NOE cross-peak intensities are measured (unpublished results).

The aqueous solution spectrum of duplex dATGCAT has been partially assigned (Patel & Tonelli, 1975), and we have confirmed these assignments, except for the thymidine 5-methyl resonances. At 10 °C, we find the terminal thymidine 5-CH_3 (T_t^5, 1.396 ppm) resonance downfield from the internal thymidine 5-CH_3 (T_i^5, 1.263 ppm) by observation of NOE's from their corresponding H6 protons. At NMR concentrations

Table I: Resonance Assignments of Duplex dATGCAT

resonance[a] (ppm)[b]			
A_i^8 (8.310)	A_t^8 (8.129)	G^8 (7.895)	A_i^2 (7.872)
A_t^2 (7.825)	C^6 (7.371)	T_i^6 (7.334)	T_t^6 (7.236)
$A_i^{1'}$ (6.295)	$A_t^{1'}$ (6.170)	$T_t^{1'}$ (6.111)	$G^{1'}$ (5.905)
$T_i^{1'}$ (5.695)	$C^{1'}$ (5.650)	C^5 (5.394)	T_t^5 (1.396)
T_i^5 (1.263)			

[a] For nomenclature, see Table II, footnote *a*. [b] Chemical shift downfield from TSP.

(~4 mM in strands), the melting point is observed at ~40 °C by measurement of the base proton chemical shift dependence on temperature. However, chemical shifts continue to change down to 15 °C due to fraying of the internal and terminal AT base pairs. Thus, all NMR observations of the duplex form were done at 10 °C to minimize such effects. At this temperature, all three imino resonances can be observed in 90% H_2O/10% D_2O. By use of the base proton assignments—confirmed by several techniques (temperature dependence of chemical shifts, deuterium exchange of purine H8, base–base NOE contacts)—the anomeric protons can be assigned by examination of the base proton–anomeric proton NOE patterns found in the 2D NOESY spectrum (Scheek et al., 1983). Thus, only one contact is found between A_t^8 and the anomeric proton region and is assigned to $A_t^{1'}$. The T_i^6 peak shows a strong NOE to another anomeric peak and a weaker NOE to the $A_t^{1'}$ peak. All of the anomeric protons are clearly assigned with this technique. Assignments to the 2',2'' and 3' deoxyribose protons can be made by examination of the COSY spectrum (Feigon et al., 1982). Resolution of the 4' and 5',5'' resonances is not adequate at 10 °C for their assignment. Assignments for the downfield part of the free dATGCAT spectrum (Figure 2) are found in Table I. Duplex dATGCAT forms a structure consistent with a B family type upon analysis of NOE intensities measured by NOESY spectra.

Assignment of the resonances in the complex ACTD–dATGCAT (1:2) (COMP2) proceeded as follows. Spectra were taken of COMP2, the complex ACTD–dATGCAT (1:4) (COMP3), and free dATGCAT at 45 °C where saturation transfer was observable. Saturation-transfer experiments on COMP3 established assignments for bound dATGCAT protons in the aromatic region (6.5–8.5 ppm) when correlated to the previously assigned resonances of free dATGCAT. The two aromatic protons of bound ACTD are strongly *J* coupled (7.4 Hz) and were assigned via the two-dimensional COSY spectrum of COMP2, which also confirmed the assignment of the cytosine H6 and H5 protons. Remaining assignments for COMP2 were done by examination of the two-dimensional COSY and NOESY spectra acquired at 15 °C, in conjunction with chemical shift considerations. A contour plot of the aromatic portion of the NOESY spectrum is shown in Figure 3. Strong NOE cross peaks are observed between base protons and the anomeric protons (5.2–6.4 ppm) of their deoxyribose moieties, with weaker cross peaks observed to the anomeric proton of the neighboring nucleotide on the 5' side. Once assignments were made of the anomeric protons, assignments could be made via the COSY spectrum and NOESY spectrum of the remaining deoxyribose protons. Assignments of the bound ACTD resonances proceeded in the same fashion. Spin systems were identified by using the COSY spectrum. Chemical shifts of ACTD pentapeptide resonances in the complex did not shift relative to free ACTD by more than 0.1 ppm, whereas chromophoric resonances shifted dramatically.

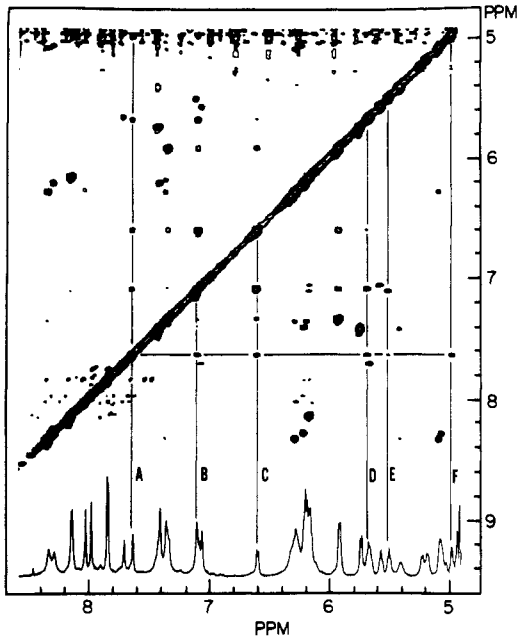

FIGURE 3: Contour plot of the ACTD–dATGCAT (1:2) NOESY spectrum. See text for experimental conditions. Peak assignments: A, guanine H8, benzenoid side of chromophore (G^8_b); B, internal thymine H6, benzenoid side of chromophore (T^6_{ib}); C, actinomycin H7; D, guanosine 1′($G^{1'}_b$); E, internal thymine 1′($T^{1'}_{ib}$); F, guanosine 3′($G^{3'}_b$).

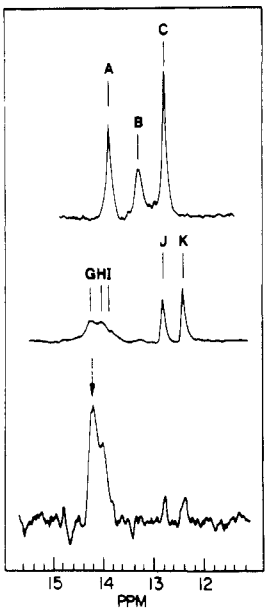

FIGURE 4: 500-MHz ^{1}H NMR spectra of imino protons. See text for experimental details. (Top) Free dATGCAT (4.0 mM strand) assignments: A, internal thymine H3 (T^3_i, 13.77 ppm); B, terminal thymine H3 (T^3_t, 13.21 ppm); C, guanine H1 (G^1, 12.69 ppm). (Middle) ACTD (4.0 mM)–dATGCAT (1:2) assignments: G, internal thymine H3, benzenoid side of chromophore (T^3_{ib}, 14.23 ppm); H, internal thymine H3, quinoid side of chromophore (T^3_{iq}, 13.95 ppm); I, terminal thymine H3 (T^3_t, 13.8 ppm); J, guanine H1, benzenoid side of chromophore (G^1_b, 12.75 ppm); K, guanine H1, quinoid side of chromophore (G^1_q, 12.34 ppm). (Bottom) NOE difference spectrum of ACTD–dATGCAT (1:2) with on-resonance irradiation (14.2 ppm) and off-resonance irradiation (11.0 ppm). Peak H (T^3_{iq}) was partially saturated as well due to peak overlap. Negative NOE's (~1%) are observed to the guanine H1 resonances, as well as to the adenine H2 resonances (not shown). Imino assignments were made by order of fraying with increasing temperature and NOE observations to previously assigned A^2 protons.

The ACTD H7 resonance and 6-CH_3 resonance were assigned by the strong NOE cross peak from one of the ACTD chromophore protons (δ = 6.60 ppm) to the large singlet at 1.97 ppm. The ACTD 4-CH_3 group was located by the strong NOE observed between the 6-CH_3 singlet (1.97 ppm) and the large singlet at 1.62 ppm. Thus, all the nonexchangeable proton resonances of this system have been located and assigned.

The major structural features of this complex can be qualitatively determined by relative NOE intensities between the assigned resonances. Spin–lattice relaxation measurements indicate a correlation time of 2–3 ns, consistent with the observed negative NOE manifested as positive cross-peak intensity in the two-dimensional experiment. The overall motion of the complex is expected to be fairly isotropic, as the model derived from our data yields overall dimensions of the complex of ~21 Å × 21 Å × 16 Å. One-dimensional TOE measurements (Wagner & Wüthrich, 1979) on several resonances of the complex showed that the time dependence of the NOE buildup rates was not influenced by spin diffusion during irradiation times less than 0.5 s. Therefore, relative proton–proton distances derived from normalized cross-peak intensities should be fairly accurate. A full treatment of our data using calculation of distances from the relaxation matrix (Macura & Ernst, 1980) and structural determination by a distance geometry algorithm (Kuntz et al., 1979) will be published later. Comparison of relative observed dynamic NOE intensities to proton–proton distances of a model (T. Lybrand and P. A. Kollman, personal communication), derived by empirical energy minimization of the originally proposed model (Sobell & Jain, 1972), shows good agreement (Table II). Over 40 ACTD to dATGCAT contacts are observed, which impose a large constraint on the possible structure of the complex.

Observation of NOE's among aromatic protons of the drug chromophore and oligonucleotide (Figure 3) demonstrates that the drug is intercalated between the GC base pairs (Table II). Table II also shows other important ACTD–dATGCAT contacts. Close contacts within the ACTD pentapeptide lactones (Table II) indicate that the structure does not radically change between the free and bound state. The large NOE's observed between Pro H_α and Dva H_α, Sar H_α indicate that the Val–Pro and Pro–Sar peptide bonds remain in the cis configuration. The close contact between Nmv N-CH_3 and the adenosine (internal) H2 protons indicates that the Sar–Nmv peptide bond most likely remains trans. The configuration of the Nmv residue may have been altered slightly upon binding, but a firm conclusion can be made only after more thorough treatment of the data by relaxation matrix and distance geometry analysis. Our data indicate that binding of the ACTD molecule to dATGCAT does not grossly alter the peptide bond configuration from that found in the aqueous free drug or the crystal structure. Thus, it appears that the mechanism underlying the slow DNA binding kinetics of ACTD involves processes different from those proposed previously (Muller & Crothers, 1968; Shafer et al., 1980; Sobell, 1974).

The structure of the bound oligonucleotide is slightly perturbed apart from the GC base pairs at the intercalation site where major changes are observed. Generally, base proton to 5′-neighboring nucleotide deoxyribose 1′,2′,2″ contacts are diminished with respect to the free dATGCAT duplex, indicating a shift in the stacking of the bases, although the structure remains within the B family.

Observation of the imino proton resonances of the bases (Figure 4) indicates that the helix stability is maintained upon drug binding. Assignment of the imino protons could be made by the NOE's observed to nonexchangeable adenine H2 protons. NOE's observed between the AT internal base pair imino

Table II: Selected Dynamic NOE Values and Distances

resonance[a] (ppm)	resonance[a] (% NOE)[b] [distance (A)][c]						
			ACTD–dATGCAT Contacts				
H8 (7.086)	G^{8}_{b} (2.4) [4.7]	C^{5}_{b},$C^{1'}_{b}$ (4.0) [4.0]	$G^{1'}_{b}$ (4.5) [3.8]	$G^{2'}_{b}$ (5.1) [1.6]	$G^{2''}_{b}$ (3.3) [2.7]		
H7 (6.600)	G^{8}_{b} (2.8) [3.6]	C^{6}_{b} (2.7) [3.8]	C^{5}_{b},$C^{1'}_{b}$ (5.2) [3.0]	$G^{1'}_{b}$ (1.4) [5.0]	$G^{2'}_{b}$ (2.0) [2.5]	$G^{2''}_{b}$ (1.4) [4.2]	
6-CH_3 (1.969)	G^{8}_{b} (3.0) [≃4.5]	C^{5}_{b},$C^{1'}_{b}$ (1.0) [4.2]					
4-CH_3 (1.624)	G^{8}_{q} (2.3) [≃4.3]						
Thrγ (1.396)	$G^{1'}_{b}$ (5.4) [≃4.0]	$G^{2'}_{b}$ (1.2) [≃3.8]	$G^{2''}_{b}$ (1.5) [≃2.6]	$C^{5'}_{b}$,$^{5''}$ (3.3) [3.4]			
A^{2}_{iq} (8.027)	Sarα_1 (1.1) [3.5]	Sarα_2 (1.3) [3.2]	Nmv N-CH_3 (10.9) [≃2.2]	Nmvγ_2 (0.6) [≃4.6]			
Pro$\beta_{2,}\gamma$ (1.834)	$C^{1'}_{b}$ (3.1) [≃2.5]						
			ACTD–ACTD Contacts				
H8 (7.086)	Thrγ (4.9) [≃2.7]						
Proα_1 (6.311)	Sarα_1 (6.7) [3.3]	Sarα_2 (7.0) [1.6]	Dvaα (16.9) [2.2]	Proβ_1 (11.2) [2.3]	Pro$\beta\gamma$ (4.9) [≃3.2]		
Thrβ_1 (5.225)	Thrα (9.6) [2.5]	Thrγ (19.6) [≃2.7]	Dvaγ_1 (15.3) [≃3.3]				
			dATGCAT Self-Contacts				
A^{8}_{iq} (8.332)	$A^{1'}_{iq}$ (6.5) [3.9]	$C^{1'}_{q}$ (1.5) [3.4]	$A^{3'}_{iq}$ (4.2) [4.2]	$A^{2'}_{iq}$,$^{2''}$ (8.2) [3.5, 2.1]	$C^{2'}_{q}$ (2.1) [2.1]	T^{5}_{t} (7.2) [4.0]	
A^{8}_{t} (8.145)	$A^{1'}_{t}$ (8.0) [3.9]	$A^{5',5''}_{t}$ (2.3) [4.0]	$A^{2'}_{t}$ (1.8) [3.7]	$A^{2''}_{t}$ (3.9) [2.1]	T^{5}_{i} (2.0) [3.5]		
G^{8}_{b} (7.634)	T^{6}_{i} (2.0) [4.8]	$G^{1'}_{b}$ (3.0) [3.9]	$T^{1'}_{i}$ (1.0) [3.9]	$G^{2'}_{b}$ (5.9) [4.4]	$G^{2''}_{b}$ (9.2) [3.4]	$T^{2'}_{ib}$ (2.6) [2.0]	$T^{2''}_{ib}$ (2.7) [2.9]
T^{6}_{tq} (7.408)	A^{8}_{iq} (1.5) [5.0]	$A^{1'}_{iq}$ (1.9) [3.3]	$T^{1'}_{t}$ (2.8) [3.7]	$T^{2',2''}_{t}$ (7.7) [3.5, 2.0]	$A^{2',2''}_{iq}$ (4.3) [2.5, 4.2]	T^{5}_{tq} (10.5) [3.0]	
C^{6}_{q} (7.392)	C^{5}_{q} (15.8) [2.5]	$C^{1'}_{q}$ (2.4) [3.7]	$C^{3'}_{q}$ (2.1) [3.8]	$C^{5'}_{q}$ (1.3) [3.6]	$C^{2''}_{q}$ (7.5) [3.6]	$C^{2'}_{q}$ (8.9) [2.0]	
T^{6}_{iq} (7.059)	A^{8}_{t} (0.4) [4.4]	G^{8}_{q} (0.5) [4.6]	$A^{1'}_{t}$ (1.4) [3.6]	$T^{1'}_{iq}$ (2.4) [3.7]	$A^{2'}_{t}$ (2.2) [2.4]	$A^{2''}_{t}$ (1.5) [3.2]	$T^{2'}_{i}$ (2.6) [3.8]

[a] Nomenclature: for $dA_tT_iGCA_iT_t$, G^{8}_{b} is guanine H8, strand on benzenoid side of ACTD chromophore; A^{2}_{iq} is internal adenine H2, strand on quinoid side of ACTD chromophore. [b] Intensity as percent of summed intensities observed along ω_1 or ω_2. [c] Calculated from energy-minimized model (see text).

protons and the GC base pair imino protons corroborate the intact nature of the helix. The conformation of the duplex is indeed altered slightly due to the ACTD chromophore intercalation between the GC base pairs and an unwinding of the helix, but we observe no major changes in the helix geometry. The integrity of the double helix in the ACTD complex implies a classical intercalation structure rather than a pseudointercalated complex recently observed with d(GpC) (Takusagawa et al., 1982). Preliminary X-ray crystallographic analysis of the same complex strongly indicates classical intercalation (H. Berman, personal communication), in agreement with our solution studies.

In summary, the salient features of this complex are as follows: (1) The ACTD chromophore is intercalated between the GC base pairs via the minor groove of the helix. (2) The structure of the ACTD pentapeptide lactones remains essentially the same for free and bound drug and is similar to that found in the crystal structure. (3) The helix geometry is perturbed slightly, but the duplex remains intact. A full analysis will be published shortly that may allow a judgment as to whether our data are complete and sufficient to determine a single, unique structure. While it is possible that our results are consistent with other structures, it is clear that they are in agreement with the originally proposed model (Sobell & Jain, 1972).

Acknowledgments

Thanks are due to G. Matson, J. Dallas, and V. Basus for their assistance with the NMR experiments.

Registry No. Actinomycin D–dATGCAT complex, 53360-01-3.

References

Angerman, N. S., Victor, T. A., Bell, C. L., & Danyluk, S. S. (1972) *Biochemistry 11*, 2402.

Bax, A., Freeman, R., & Morris, G. (1981) *J. Magn. Reson. 42*, 164.

Braun, W., Bosch, C., Brown, L. R., Gō, N., & Wüthrich, K. (1981) *Biochim. Biophys. Acta 667*, 377.

Brown, S. C., Shafer, R. H., & Mirau, P. A. (1982) *J. Am. Chem. Soc. 104*, 5504.

Davanloo, P., & Crothers, D. M. (1976) *Biochemistry, 15*, 5299.

Feigon, J., Wright, J. M., Leupin, W., Denny, W. A., & Kearns, D. R. (1982) *J. Am. Chem. Soc. 104*, 5540.

Jain, S. C., & Sobell, H. M. (1972) *J. Mol. Biol. 68*, 1.

Krugh, T. R., & Chen, Y. C. (1975) *Biochemistry 14*, 4912.

Kuntz, I. D., Crippen, G. M., & Kollman, P. A. (1979) *Biopolymers 18*, 939.

Macura, S., & Ernst, R. R. (1980) *Mol. Phys. 41*, 95.

Mauger, A. B. (1980) *Top. Antibiot. Chem. 5*, 229.

Mirau, P. A., & Shafer, R. H. (1982) *Biochemistry 21*, 2626.

Muller, W., & Crothers, D. M. (1968) *J. Mol. Biol. 35*, 251.

Narang, S. A., Brousseau, R., Hsiung, H. M., & Michniewicz, J. (1980) *Methods Enzymol. 65*, 610.

Patel, D. J. (1974a) *Biochemistry 13*, 2388.

Patel, D. J. (1974b) *Biochemistry 13*, 2396.

Patel, D. J., & Tonelli, A. E. (1975) *Biochemistry 14*, 3990.

Patel, D. J., Kozlowski, S. A., Rice, J. A., Broka, C., & Itakura, K. (1981) *Proc. Natl. Acad. Sci. U.S.A. 78*, 7281.

Plateau, P., & Gueron, M. (1982) *J. Am. Chem. Soc. 104*, 7310.

Reid, D. G., Salisbury, S. A., & Williams, D. H. (1983) *Biochemistry 22*, 1377.

Reinhardt, C. G., & Krugh, T. R. (1977) *Biochemistry 16*, 2890.

Scheek, R. M., Russo, N., Boelens, R., & Kapstein, R. (1983) *J. Am. Chem. Soc. 105*, 2914.

Shafer, R. H., Burnette, R. R., & Mirau, P. A. (1980) *Nucleic Acids Res. 8*, 1121.

Sobell, H. M. (1974) *Cancer Chemother. Rep., Part 1 58*, 101.

Sobell, H. M., & Jain, S. C. (1972) *J. Mol. Biol. 68*, 21.

States, D. J., Haberkorn, R. A., & Ruben, D. J. (1982) *J. Magn. Reson. 48*, 286.

Takusagawa, F., Dabrow, M., Neidle, S., & Berman, H. (1982) *Nature (London) 296*, 466.

Wagner, G., & Wüthrich, K. (1979) *J. Magn. Reson. 33*, 675.

Wüthrich, K., Wider, G., Wagner, G., & Braun, W. (1982) *J. Mol. Biol. 155*, 311.